Multi-line superconducting waveguides based on YBCO-on-Kapton technology

Vyacheslav Solovyov, Hyunwoo Kim, and Paul Farrell

***Abstract*— Coplanar (with the ground) and stripline 25 cm long waveguides are manufactured from the YBCO-Kapton material. The waveguides are intended as the key components of a scalable signal delivery for large quantum computing systems and detectors. The waveguide is coupled with an integrated power divider that replaces the standard attenuator. The divider is designed to return most of the power to the previous thermalization stage. The method is projected to reduce the active dissipation by ≈ 10. We investigate the effect of internal strain in YBCO layer on the device's mechanical stability. We show that adhesives with high stiffness are essential for the reliability of YBCO-Kapton devices.**

***Index Terms*— High-temperature superconductors, quantum computing, RF properties, scalable interface.**

I. Introduction

SCALING of the superconducting quantum computing systems (sQS) requires overcoming several technological challenges. A large number of physical elements, or qubits, need to be synchronized, pre-set, manipulated, and readout to perform an error-free quantum computation. Input-output is considered a bottleneck of a quantum computer system that limits communication of the quantum processor with the room temperature environment. A single qubit typically needs up to three control lines and one readout line. Multiqubit architectures with tunable couplers require extra control lines. The flux control lines cannot be multiplexed, while strict bandwidth and crosstalk requirements limit the microwave signal multiplexing. The sQS wiring accounts for the most significant part of the heat load in a large quantum system.

It is well-recognized that passive loss (thermal conduction of cables) accounts for approximately 50% of the heat load of a typical quantum computer [1]. The remaining 50% is the active loss due to the dissipation of electric signals in resistive attenuators. Attenuation, 60 dB total, is needed to guarantee a noise photon number below the 10^{-3} level. A scalable quantum interface should thus mitigate sources of both active and passive heat loads without adding thermal noise. Several solutions are considered to address the interface scalability in superconducting quantum systems [2, 3].

Previously, we have demonstrated RF waveguides based on the so-called YBCO-Kapton technology [4, 5]. The technology uses epitaxial films of high-temperature ceramic superconductor YBCO as the conducting trace and Kapton as the dielectric substrate. The ultra-low thermal conductivity of YBCO-Kapton material can potentially reduce the conduction loss between 30 K and 10 mK by at least ×100, compared with the standard 2 mm stainless steel coaxial lines. We propose leveraging this feature of the YBCO-Kapton technology to address the active loss in attenuators. A power divider with a power return line can be realized with negligible passive loss penalty and practically eliminate active dissipation at the critical cold plate and mixing chambers; see, for example, Fig. 1. Here, at every thermalization stage, the power is split by a 20 dB divider, but instead of dissipation of the 99% power at the attenuator, it is returned to the previous stage via an impedance-matched return line and dissipated onto a 50 Ω load. A simple resistive power splitter

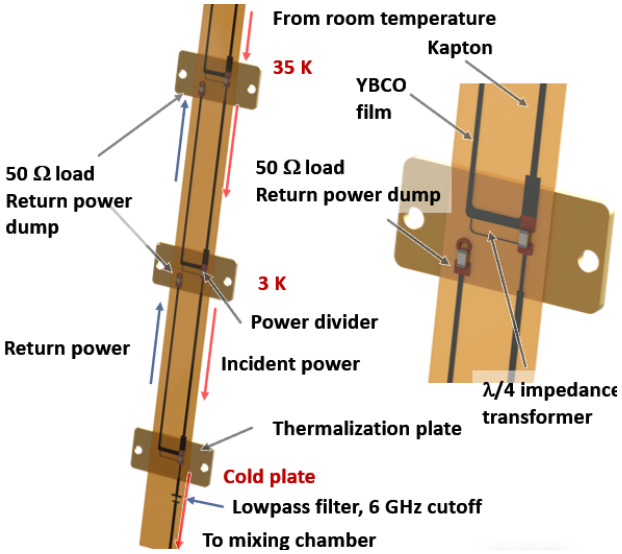

Fig. 1. Rendering of the proposed microwave drive line. The microwave power is divided at each thermalization stage by a 20 dB power divider. The unused power is returned to an upstream thermalization stage via a power return line. The right panel shows the realization of the power split with an unequal Wilkinson divider. Here, the ground planes have been removed for clarity.

would deliver ×10 lower active dissipation. Ultimately, a Wilkinson-type divider [6] with λ/4 impedance transformers would further reduce the active loss.

In this work, we demonstrated the key elements of the proposed scalable signal delivery: the low-loss shielded stripline waveguide and resistive power divider with a power return line.

Manuscript received ; accepted . Date of publication; date of current version . This work was supported by U.S. DOE Office of Science award DE-SC0021707. *(Corresponding author: Vyacheslav Solovyov.)*

V. F. Solovyov is with Brookhaven Technology Group, 1000 Innovation Road, Stony Brook, NY 11794, (slowa@brookhaventech.com).

Hyunwoo Kim and Paul Farrell is with Brookhaven Technology Group, 1000 Innovation Road, Stony Brook, NY 11794

Color versions of one or more of the figures in this paper are available online at http://ieeexplore.ieee.org.

Digital Object Identifier

II. Experiment

The 12 mm wide YBCO films, supported by 20 μm thick copper foil, were separated (exfoliated) from the metal substrate and buffer of 2G tapes supplied by SuperPower Inc, AMSC Corp., and SuperOx, as previously described in [7]. Fig. 2a shows the YBCO side of the exfoliated coupons. Here the YBCO film was etched from approxmately half of the coupon to quantify the copressive stress of the YBCO layer. The compressive stress of the YBCO layer manifested itself as warping of the copper foil, well visible in Fig. 1a. The warp curvature varied greatly from batch to batch and from manufacturer to manufacturer, which was indicative of a large variation of the internal strain even within a conductor coupon. We achieved similar performance for YBCO films from the three manufacturers; therefore, in the following, we report only results for devices manufactured from the SuperPower tape. The YBCO-Copper foils were bonded to 2 mils (50 μm) thick Kapton tape. The standard photolithography, via drilling and via metallization processes, [4] were utilized to manufacture two-line coplanar with the ground (CPWG) and stripline-type waveguides, Fig. 2b. In this experiment, we used liquid epoxy, Stycast 1266, to bond the YBCO layer to Kapton. Trials of dry-film adhesives, such as 3M 583 and Rodgers 2929 resulted in a cracked YBCO layer, Fig. 2c. To determine the total DC resistance of the YBCO lines in the magnetic field under radiation cooling, we manufactured a sample with 1 mm wide lines and soldered current leads, Fig. 2d. The current lead area was ≈ 2 mm^2. The sample were tested in a conduction-cooled vacuum chamber at 30 K and in magnetic field up to 1 Tesla, field ramp 2 mT/s

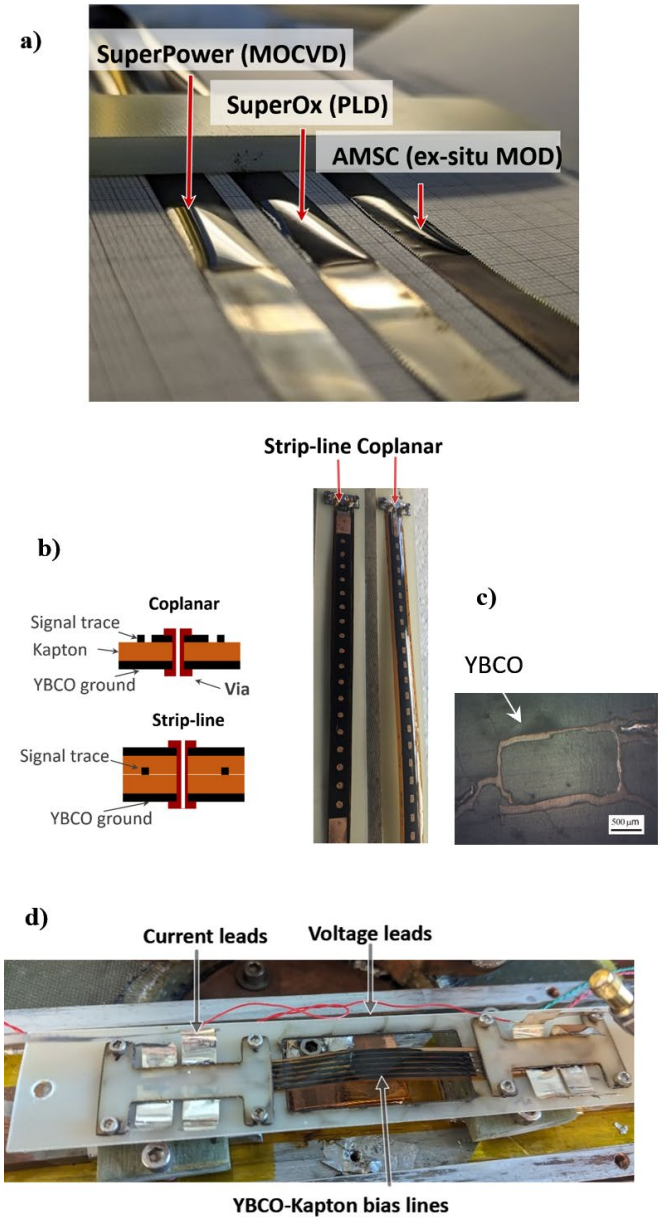

Fig. 2. a) Coupons of YBCO-Copper foils exfoliated from SuperPower, SuperOx and AMSC 2G conductors. The YBCO layer was etched from a part of the coupon to demonstrate the warping of copper foil due to the compressive strain of the YBCO film. b) 25 cm long, two-line coplanar and stripline waveguides. The insert is a schematic rendering of the waveguides cross-sections. c) Optical micrograph of YBCO layer bonded with 3M 583 thermoset film. d) 1 mm wide DC bias lines in a thermalization enclosure for radiation-cooling test.

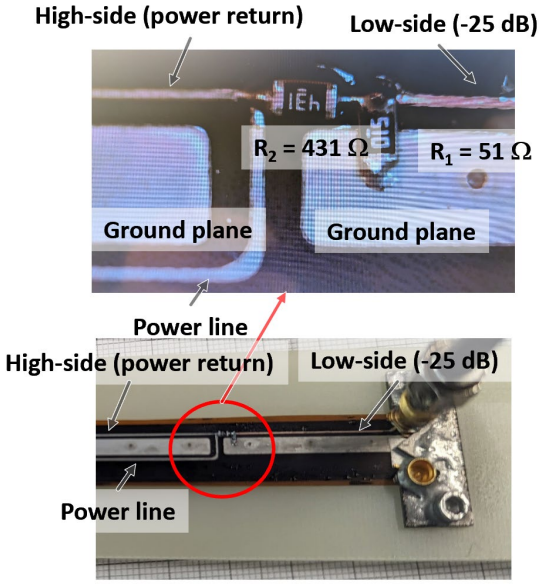

Fig. 3. Realization of resistive power divider with a power return line on a 25 cm long coplanar with ground waveguide. The power is divided by a pair of series-connected 431 Ω and 51 Ω resistors, as shown in the upper panel. 99% of the power is returned via a return line to a 50 Ω termination.

Fig. 3 shows the realization of a resistive power divider concept, presented in Fig. 1, in a 25 cm long CPWG waveguide. Here, surface-mounted resistors (0603 size) were soldered directly on the waveguide signal lines using Sn63Pb37 solder. The resistivity ratio (431 Ω and 51 Ω) was chosen to yield approximately 25 dB attenuation. The return line was terminated with a 50 Ω resistor at the input connector. The waveguide was connectorized with surface-mounted SMP connectors Molex WM3891TR. The waveguides were tested at 77 K in liquid Nitrogen using a Signal Hound scalar network analyzer comprised of a TG-124A generator and SA-124B spectrum analyzer.

III. Results

Fig. 4a compares the insertion loss, S_{21}, of 25 cm CPWG, and stripline waveguides at room temperature and 77 K. In the superconducting state, 77 K, the waveguides demonstrate < 0.5 dB loss at 6 GHz. The waveguides are calculated to be impedance-controlled 50 Ω; however, the S_{21} spectrum oscillations indicate the impedance mismatch. Further, the time domain reflectometry measurements placed the actual waveguide impedance at 40 Ω. The discrepancy is explained by the difference in dielectric constants of the Kapton substrate and epoxy adhesive,

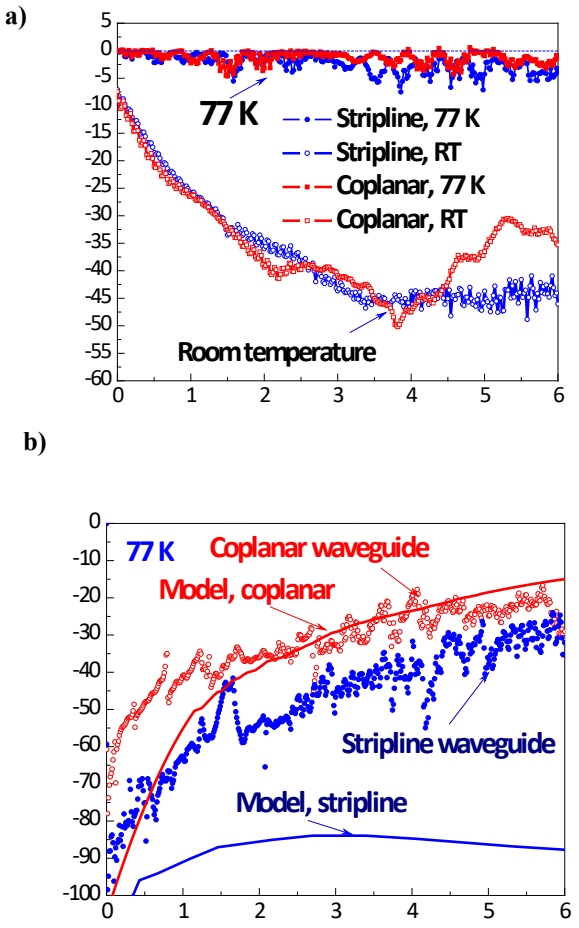

Fig. 4. a) Insertion loss, S_{21}, of coplanar and stripline waveguides at room temperature and 77 K. b) Near-end cross-talk of the coplanar and stripline waveguide at 77 K. The solid lines are numeric simulations using Sonnet RF Suite.

Stycast 1266, that we used to bond YBCO to Kapton. Fig. 4b presents near-end cross-talk spectra for the two waveguides. The solid lines are numeric simulations of the waveguides performed in the Sonnet RF suite.

Fig. 5 is a result of DC line resistance measurement in the radiation cooling mode. The 1 mm wide YBCO line is excited with a DC current up to 400 mA, and the current is maintained for over 1 hr. The total line resistance (including contacts) is 1.5 μΩ, which corresponds to the contact areal resistivity of 50 nΩ cm^2. The line remains superconducting in a magnetic field up to 1 Tesla without any change in resistivity.

Fig. 5 demonstrates the performance of the 25 dB power divider shown in Fig. 3, 77 K. The plot shows the S_{21} spectrum of both power return and the attenuated signals. The power return spectrum is recorded between the power input and the power return ports.

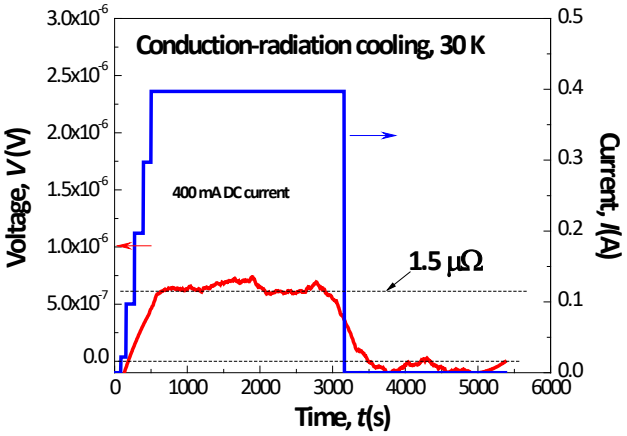

Fig. 5. Test of 1 mm wide DC bias line, shown in Fig. 2d, under radiation cooling, 30 K. The line is excited to the maximum current 400 mA. The horizontal line indicates the average line resistance of 1.5 μΩ.

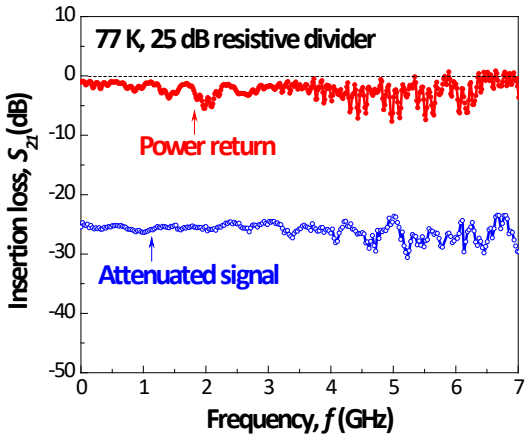

Fig. 6. Performance of resistive power divider shown in Fog. 3. The "high side" is the spectrum recorded between the power input and the power return ports. The "low side" is the spectrum of the attenuated signal after the resistive divider.

IV. Discussion

Table 1 compares the projected active (attenuator) and passive (thermal conduction) loss of the traditional microwave signal delivery setup and the proposed technology. The traditional signal delivery is realized by UT-085-SS-SS (Micro-Coax Inc.) coaxial cables coupled to 20 dB thermalized t-pad attenuators. The proposed solution is comprised of 20 dB resistive dividers integrated into a YBCO-Kapton stripline, as shown in Fig. 3. If implemented in a large quantum computing system, the proposed technology is expected to reduce the active attenuator

TABLE I
PROJECTED LOSS OF THE TRADITIONAL SIGNAL DELIVERY AND YBCO-KAPTON STRIPLINE

	Active loss at the attenuator, 10 dBm CW		Conduction (passive) loss	
Stage	20 dB attenuators	**20 dB resistive power divider**	Drive line UT-085-SS-SS	**YBCO-Kapton stripline**
50 K			45 mW	0.9 mW
4 K	10 mW	0.9 mW	1.8 mW	0.078 mW
100 mK	100 μW	1.1 μW	0.25 μW	0.013 μW
10 mK	1 μW	0.11 μW	1.0×10^{-9} W	2.9×10^{-11} W

loss by ×10 and the passive loss by the factor of > 20, for a 5 mm pitch waveguide discussed in this work. Fig. 4 demonstrates that YBCO-Kapton waveguides, both CPWG and stripline type, can be manufactured in lengths relevant to a typical cryogenic system. In a stripline waveguide, the signal lines are sandwiched by the ground panes, which can yield much better inter-line isolation than a coplanar waveguide. Indeed, in Fig. 4b, we observe, on average, 20 dB better cross-talk in the stripline waveguide compared to the CPWG. However, the absolute level of cross-talk is still higher than predicted by a numeric model, indicating that the waveguide transition to SMP connectors needs further improvement. We note that extra passive elements in a resistive divider, Fig. 3, do generate their own thermal noise current and thus elevate the noise level. However, a simple estimate shows that the divider is expected to elevate the noise level by only 15% over a standard t-pad attenuator.

The very low contact resistance of Silver-YBCO interface, Fig. 5, enables efficient delivery of both DC and RF bias currents in variable frequency qubit processors and cryogenic detectors. The high-energy physics detectors often operate in high magnetic fields. YBCO is a type-2 superconductor with strong magnetic flux pinning and high critical current, which entails high magnetization (AC) loss. Our estimate, based on the Brandt model [8], predicts that a 10 mm wide YBCO-Kapton line suspended in vacuum and surrounded by a 4 K radiation shield would be able to sustain AC loss at the maximum magnetic field ramp rate of 5 mT/s before quenching.

The realization of multi-layer YBCO depends on a reliable transfer of the ceramic epitaxial layer onto a soft polymeric substrate while retaining the integrity of the brittle superconducting film. We identify the built-in compressive stress of the YBCO film as a factor that is responsible for YBCO film failure after the transfer. The YBCO stress level varies greatly within the same batch of 2G tape, which suggests that the local material structure, such as grain size, contributes the most. We found that YBCO layers with large, > 10 μm, grains, such as those manufactured by the ex-situ process employed by AMSC, have the least amount of stress, see also Fig. 2a. On the other side of the spectrum, small-grain (< 1 μm) YBCO grown by a physical method, for example, pulsed-laser deposition (SuperOx), has the highest level of compression. The grain size has long been associated with intrinsic stress in both metal and ceramic films [9, 10]. The so-called Stoney formula [11] estimates the film's stress from the measured substrate curvature κ [12]:

$$\sigma \approx \frac{E h_s^2 \kappa}{6 h_f} \quad (1)$$

Here E is the Young's modulus of the substrate, and h_s and h_f are the thicknesss of the film and the substrate, correspondingly. Taking typical numbers for the copper stabilizer layer, E = 110 GPa, h_s = 20 μm, and h_f = 1 μm for YBCO, we arrive at σ = 290 MPa for the SuperPower YBCO. This level of stress does not pose a problem when the YBCO film is constrained by thick and rigid substrates, such as Hastelloy with E = 220 GPa. However, the polymeric substrates, such as Kapton, are much softer, E = 2.5 GPa. The elastic model of a stressed rigid film on a compliant substrate predicts that such an arrangement is prone to buckling instabilities [13]. When the buckling stress exceeds the mechanical limit of the film material, the film is expected to fail by cracking. The buckling instability and the following film failure occur at the critical strain level:

$$\varepsilon_c = \frac{1}{4}\left(\frac{3E_s}{E_f}\right)^{2/3} \quad (2)$$

Here E_s and E_f are elastic moduli of the film and the substrate, correspondingly. A YBCO film with a compressive stress of 290 MPa can be treated as a pre-compressed layer with ε = 0.2%. If we use the YBCO value E = 138 GPa in Eq. 2 we calculate ε_c = 2.9%, meaning that if a YBCO film were directly deposited on Kapton, the buckling would not occur. In practice, there is a layer of soft adhesive between the YBCO film and the Kapton tape. Our experiments show that it is the mechanical properties of the adhesive that most affect the YBCO film's integrity. Our attempts to use popular dry-film adhesives, such as 3M 583 with E_s < 0.1 GPa, resulted in cracked YBCO films, as shown in Fig. 2c. This is explained by the YBCO film strain, 0.2%, exceeding the critical value, 0.07%, predicted by Eq. 2 for 3M 583 adhesive. Even though the dry film adhesives are very convenient to use, they tend to have low stiffness, which leads to cracking of the YBCO film. So far, only high-performance liquid adhesives, such as Stycast 1266, have demonstrated stiffness that is high enough to withstand the compressive stress of the YBCO layer.

V. CONCLUSION

In conclusion, we demonstrated components of a scalable microwave interface using three-layer stripline waveguides YBCO-Kapton material with integrated power dividers. The remaining challenge of the technology is identifying a dry-film adhesive compatible with highly strained YBCO films. Future work will focus on the integration of low-bandpass and IR filters into the waveguide structure.

REFERENCES

[1] S. Krinner, S. Storz, P. Kurpiers, P. Magnard, J. Heinsoo, R. Keller, J. Lütolf, C. Eichler, and A. Wallraff, "Engineering cryogenic setups for 100-qubit scale superconducting circuit systems," *EPJ Quantum Technology,* vol. 6, no. 1, p. 2, 2019/05/28 2019, doi: 10.1140/epjqt/s40507-019-0072-0.

[2] J. P. Smith, B. A. Mazin, A. B. Walter, M. Daal, I. J. I. Bailey, C. Bockstiegel, N. Zobrist, N. Swimmer, S. Steiger, and N. Fruitwala, "Flexible Coaxial Ribbon Cable for High-Density Superconducting Microwave Device Arrays," *IEEE Trans. Appl. Supercond.,* vol. 31, no. 1, pp. 1-5, 2021, doi: 10.1109/TASC.2020.3008591.

[3] A. Shah, V. Gupta, B. Yelamanchili, S. E. Peek, M. F. F. Chowdhury, A. S. Rashid, U. S. Goteti, J. A. Sellers, D. B. Tuckerman, and M. C. Hamilton, "Towards Cable-to-Cable Connectors for Flexible Thin-Film Superconducting Transmission Lines," *IEEE Trans. Appl. Supercond.,* vol. 31, no. 5, pp. 1-6, 2021, doi: 10.1109/TASC.2021.3062566.

[4] V. Solovyov, H. Kim, and P. Farrell, "High-Temperature Superconducting Interconnects for Ultra-Low Temperature, High-Field Environments," *IEEE Trans. Appl. Supercond.,* vol. 33, no. 5, pp. 1-5, 2023, doi: 10.1109/TASC.2023.3241264.

[5] V. Solovyov, O. P. Saira, Z. Mendleson, and I. Drozdov, "YBCO-on-Kapton: Material for High-Density Quantum Computer Interconnects With Ultra-Low Thermal Loss," *IEEE Trans. Appl. Supercond.,* vol. 31, no. 5, pp. 1-5, 2021, doi: 10.1109/TASC.2021.3057010.

[6] D. M. Pozar, *Microwave engineering*. John wiley & sons, 2011.

[7] V. Solovyov and P. Farrell, "Exfoliated YBCO filaments for second-generation superconducting cable," *Supercond. Sci. Technol.,* vol. 30, no. 1, p. 014006, 2017. [Online]. Available: http://stacks.iop.org/0953-2048/30/i=1/a=014006.

[8] E. H. Brandt and M. Indenbom, "Type-II-superconductor strip with current in a perpendicular magnetic field," *Phys. Rev. B,* vol. 48, no. 17, p. 12893, 1993. [Online]. Available: http://link.aps.org/doi/10.1103/PhysRevB.48.12893.

[9] Z. Rao, S. J. Hearne, and E. Chason, "The Effects of Plating Current, Grain Size, and Electrolyte on Stress Evolution in Electrodeposited Ni," *J. Electrochem. Soc.,* vol. 166, no. 1, pp. D3212-D3218, 2018/12/06 2018, doi: 10.1149/2.0261901jes.

[10] H. Lee, S. S. Wong, and S. D. Lopatin, "Correlation of stress and texture evolution during self- and thermal annealing of electroplated Cu films," *J. Appl. Phys.,* vol. 93, no. 7, pp. 3796-3804, Apr 2003, doi: 10.1063/1.1555274.

[11] G. G. Stoney and C. A. Parsons, "The tension of metallic films deposited by electrolysis," *Proceedings of the Royal Society of London. Series A, Containing Papers of a Mathematical and Physical Character,* vol. 82, no. 553, pp. 172-175, 1909, doi: doi:10.1098/rspa.1909.0021.

[12] L. B. Freund and S. Suresh, *Thin film materials: stress, defect formation and surface evolution*. Cambridge university press, 2004.

[13] H. Jiang, D.-Y. Khang, J. Song, Y. Sun, Y. Huang, and J. A. Rogers, "Finite deformation mechanics in buckled thin films on compliant supports," *Proceedings of the National Academy of Sciences,* vol. 104, no. 40, pp. 15607-15612, 2007, doi: doi:10.1073/pnas.0702927104.